Pergamon

*Int. J. Heat Mass Transfer.* Vol. 38, No. 11, pp. 2109–2115, 1995

0017-9310/95 $9.50+0.00

0017-9310(94)00324-6

# Numerical experiments on free and forced convection in porous media†

E. HOLZBECHER‡ and Y. YUSA

Kyoto University, Beppu Geophysical Research Laboratory, Oita 874, Japan

(*Received* 9 *June* 1994 *and in final form* 2 *September* 1994)

**Abstract**—Understanding the patterns of flow induced by geothermal sources in deep ground is still a problem, although the basic hydraulic regimes are identified. The interaction of flow and heat-transport results in different flow phenomena depending on the variability and range of the parameters involved. A qualitative and quantitative characterization is given in this paper.

## 1. INTRODUCTION

The focus of researchers in the past lay on convection between horizontal isothermal boundaries in a system which would be hydrostatic if the temperatures were constant on both boundaries. In fact, this is the situation of the Benard experiment with the difference that a porous medium fills the containment—not pure fluids. It was predicted by theoretical derivations [1] and confirmed by laboratory and numerical experiments that the hydrodynamical behaviour is determined by the Rayleigh number *Ra* only. If *Ra* for a specific system exceeds a critical value, convection will set in. Otherwise it will move into a hydrostatic situation.

This phenomenon is referred to as natural convection [2] or free convection. The latter term was taken from turbulent shear flow: '"free convection" occurs in a range where the contribution to the vertical transfer of momentum and heat by mechanical turbulence can be neglected compared to those carried by convection' [3]. Forced convection, in contrast, occurs when the generation of turbulence by the shear dominates over the generation by buoyancy.

In the case of porous media turbulence is mostly not relevant, but there is a similar situation of practical importance, when a hydraulic gradient at the upper boundary is introduced in a geothermal system—a situation which is referred to as combined forced and free convection [4] or mixed convection [5]. Prats [6] showed that the characteristic behaviour does not change in this case: the Rayleigh number remains the only physical parameter determining the hydrodynamics or -statics of the system.

In this paper it will be shown that this result depends on the very specific conditions of the system tackled by Prats: (1) that it is infinite and (2) that the heat source is continuously distributed on the entire lower boundary of the porous medium layer. Both conditions are never fulfilled in real systems. Numerical experiments on a finite system and a finite location of the heat source show that, in the case of forced and free convection, the hydraulic gradient has an influence on convection—additional to the influence of the Rayleigh number.

For a constant velocity field **v** Prats [6] derived solutions from the stationary cells of the free convection case under the condition that the system has infinite length. If the $x$-axis is chosen in the direction of **v** the mixed convection steady state can be derived by replacing the $x$-coordinate of the free convection solution by $x$-$vt$, i.e. by connecting with a moving coordinate system. It is obvious that this procedure cannot be applied as well when there are vertical boundaries somewhere.

## 2. REFERENCE CASE DESCRIPTION

The reference case for the calculations was a simplified but ideal typical situation presented by Yusa [7]. A confined, homogeneous and isotropic aquifer of 1000 m depth is considered. From an isothermal source at the bottom with 1000 m length, the aquifer extends 5000 m. The relevant characterizing parameters of fluid and porous medium are listed in Table 1. Fluid properties besides density were assumed to be constant. Density decrease is assumed to be linear in the temperature range between $T_0 = 20°C$ and $T_1 = 250°C$:

$$\rho = \rho_0 - \Delta\rho\Theta$$

with normalized temperature

$$\Theta = \frac{T - T_0}{T_1 - T_0}.$$

†Contribution No. 10, Foreign Visiting Scientist Section, Beppu Geophysical Research Laboratory.

‡Present address: TU Berlin, Sekr. W, P.O. Box 100 320, D-10563 Berlin, Germany.

## NOMENCLATURE

| | |
|---|---|
| $a$ | viscosity slope parameter (see below) |
| $c$ | specific heat |
| $g$ | constant of gravity |
| $\mathbf{g}$ | vector of gravity (in direction of gravity with length $g$) |
| $H$ | height |
| $k$ | permeability |
| $L$ | length |
| $t$ | time |
| $p$ | (total) pressure |
| $Ra$ | Rayleigh number (see below) |
| $T$ | temperature |
| $T_0$ | low temperature at boundary |
| $T_1$ | high temperature at boundary |
| $\mathbf{v}$ | vector of Darcy velocity (with components $v_x$, $v_z$) |
| $v_b$ | horizontal component of Darcy velocity at upper boundary |
| $x$ | horizontal space variable |
| $z$ | vertical space variable (in direction of gravity). |

Greek symbols

| | |
|---|---|
| $\gamma$ | ratio of heat capacities (see below) |
| $\Delta\rho$ | maximum density difference |
| $\Delta x$ | horizontal grid spacing (for equidistant grid) |
| $\Delta z$ | vertical grid spacing (for equidistant grid) |
| $\Phi$ | porosity |
| $\kappa$ | thermal diffusivity |
| $\mu$ | dynamic viscosity |
| $\mu_{ref}$ | reference viscosity (corresponding to $\theta_{ref}$) |
| $\theta$ | normalized temperature (see below) |
| $\theta_{ref}$ | reference normalized temperature |
| $\theta_0$ | viscosity increment parameter (see below) |
| $\rho$ | fluid density |
| $\rho_0$ | fluid density at low temperature $T_0$ |
| $\tau$ | dimensionless time |
| $\Psi$ | streamfunction. |

Subscript

| | |
|---|---|
| m | for aquifer characteristic. |

Table 1. Characteristic properties of the fluid and the aquifer

| | | |
|---|---|---|
| $H$ | height | 1000 m |
| $\Delta\rho$ | fluid density difference | 230 kg m$^{-3}$, |
| $\mu$ | dynamic viscosity | $2\times10^{-4}$ kg m$^{-1}$ s$^{-2}$ |
| $k$ | permeability | $10^{-14}$ m$^2$ |
| $\kappa$ | thermal diffusivity | $10^{-6}$ m$^2$ s$^{-1}$ |
| $\gamma$ | heat capacities ratio ($\rho c/\rho_m c_m$) | 2 |

### 3. ANALYTICAL FORMULATION

The continuity equations for flow and heat, applying Darcy's Law for fluid flow and Fourier's Law for heat flow are transformed into a set of two equations in two (dimensionless) space variables. Additionally the streamfunction $\Psi$ is introduced under the condition that the Boussinesq assumption is valid. The details are noted by Yusa [7], but it is worth mentioning an alternative time transformation:

$$t \longrightarrow \tau = t\kappa/\gamma H^2$$

where $\gamma$ appears in the denominator in contrast to Yusa's transformation rule.

This leads to the following set of equations:

$$\begin{aligned} \operatorname{div}(\operatorname{grad}\Psi) &= \gamma Ra\frac{\partial\Theta}{\partial x} \\ \operatorname{div}(\operatorname{grad}\Theta) - v\operatorname{grad}\Theta &= \frac{1}{\gamma}\frac{\partial\Theta}{\partial\tau} \end{aligned} \qquad \text{(X)}$$

with Rayleigh number $Ra$ defined as

$$Ra = \frac{kg\Delta\rho H}{\mu\kappa}.$$

The variables used in Yusa [7] transform into the ones of equations (X) as follows:

$$\tau \longrightarrow \tau/\gamma \quad \mathbf{v} \longrightarrow \mathbf{v}/\gamma \quad \Psi \longrightarrow \Psi/\gamma.$$

The steady-state equations of (X) were used first by Wooding [8], later by Elder [9] for numerical simulations. The system (X) is implemented in the finite difference code FAST_C(2D) [10], which was used for computer simulations here.

The boundary conditions in the dimensionless equations (X) are summarized in Table 2.

Taking the specified values for the parameters, the factor of time transformation is $0.5\times10^{-12}$ and the Rayleigh number becomes 113.

Variations of the reference case were made by Yusa [7] concerning the piezometric head gradient at the top of the model. In the following these will be referred to as low (1 var.), medium (2 var.) and high (3 var.) velocity variations. They are characterized by hydraulic gradients of 1, 3 or 5%, respectively, at the

Table 2. Boundary conditions for reference case of length $L$

| | Flow | Heat |
|---|---|---|
| Vertical boundaries | $\Psi = 0$ | $\frac{\partial \Theta}{\partial x} = 0$ |
| Top boundary | $\frac{\partial \Psi}{\partial z} = 0$ | $\Theta = 0$ |
| Bottom boundary | $\Psi = 0$ | $\frac{\partial \Theta}{\partial z} = 0$ for $x \varepsilon [0, L-H]$ |
| | | $\Theta = 1$ for $x \varepsilon [L-H, L]$ |

top of the aquifer. These gradients transform into specified values for $\partial\Psi/\partial z$ at the top boundary (4.9, 14.7 and 29.5 using Yusa's transformation, respectively, 9.8, 29.4 and 49.0 transforming as noted above).

## 4. SIMULATIONS WITH FAST_C(2D) CODE

The FAST_C(2D) code is based on a finite-difference–finite-volume discretization of equations (X) for two-dimensional irregular rectangular grids [10]. First-order equations are discretized by the upwind scheme. Timestepping is implemented as a generalization of the Crank–Nicolson method with a user-defined time level weighting factor. The nonlinear set of equations is solved by a Piccard inner iteration algorithm, where flow and transport are solved iteratively until a specified accuracy $\varepsilon$ is reached. The solvers for the linear systems can be chosen out of various conjugate gradient (CG) methods (here with preconditioning).

For the calculations of this paper the Crank–Nicolson method was chosen to solve the $\Theta$-equation of system (X). The calculations were done on a NEC-H9870 personal computer and execution time for all simulations was around 90 min for an inner iteration accuracy $10^{-4}$.

Numerical calculations were done with a fixed length of the aquifer ($L = 5000$ m or $L = 4000$ m). It was observed for this choice of $L$ that the far (from source) boundary condition did not have an influence on flow and temperature distributions in the vicinity of the geothermal source. Thus the change of the hydraulic boundary condition or a prolongation of the model would not alter the thermal convection pattern. The grid was chosen equidistant with $100 \times 20$ blocks for 5000 m length ($80 \times 20$ for $L = 4000$ m).

The computer model simulates the transient development of the physical model. The initial state is the hydrostatic case with constant cold temperature or $\Theta = 0$. The simulation was stopped when the system showed only marginal changes: then the solution is nearly steady state. In some cases the change of variables did not decrease, not even if the simulation time was increased: no steady state exists. The usual end of simulation time corresponds to 5000 years in real dimensions.

The results for the reference case and the variations are shown in Figs. 1–4. In Figs. 1, 2 and 4 the system is in steady state; in Fig. 3 it is transient. The pictures show streamlines (thin lines) and isotherms (thick lines). Isotherms are plotted for $\Theta$-values 0.2, 0.4, 0.6 and 0.8. Plotted streamline levels are equidistant.

Comparison with Yusa [7] shows that the results are qualitatively the same. The four cases show different flow patterns depending on the velocity prescribed at the upper boundary. They can be classified as follows:

Ref.case (zero velocity) → one steady convection cell
1 var. (low velocity) → three steady convection cells
2 var. (medium velocity)
→ fluctuating convection eddies
3 var. (high velocity) → no convection.

The transient development in the reference case shows the emergence of an ascending flow region above the heat source which moves horizontally to the closed (right) boundary, until there remains only one convection cell with hot water rising at the vertical system boundary. Both numerical simulations show this same characteristic behaviour.

In the 1 variation with prescribed low velocity at the upper boundary the ascending flow region which appears first does not move to the boundary, where instead another hot water zone emerges. In between the two ascending water regions the third convection cell with opposite rotation (clockwise) appears. One major discrepancy can be observed by comparing both simulations: in Yusa's calculations the emergence of the second ascending region is between 2000 and 3000 years, while it appears after 4000 years in FAST_C(2D) output. Results for transient and steady-state reference cases and steady-state of the 1 variation case were also well published by Yano [11]. The output of the finite-element simulation is very much the same as the ones presented here.

The 2 variation has no steady state, as both numerical simulations demonstrate. There is hot water moving with the overlying flow field. From there unstable

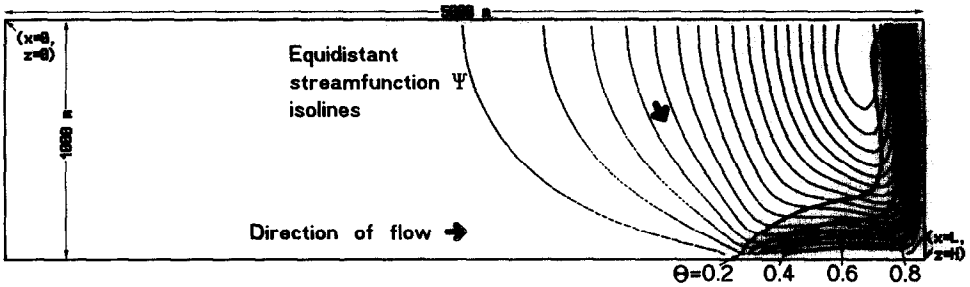


Fig. 1. Steady-state solution of reference case.

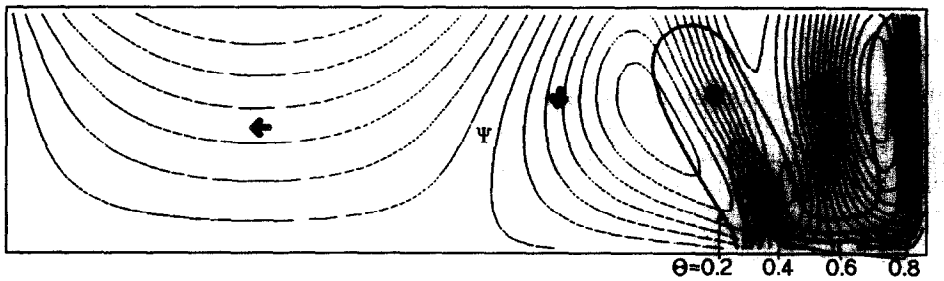


Fig. 2. Steady-state solution of 1 variation (low velocity).

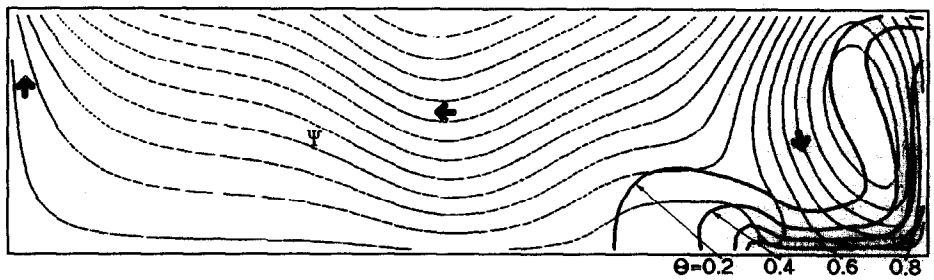


Fig. 3. Transient solution of 2 variation (medium velocity).

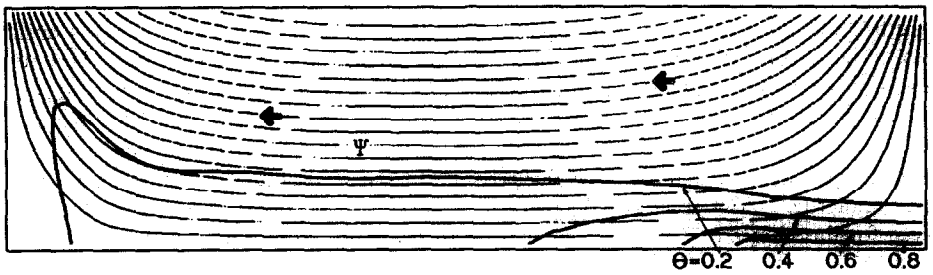


Fig. 4. Steady-state solution of 3 variation (high velocity).

hot plumes emerge. The pattern of these 'transients' is quite different in both simulations. The differences can be attributed to discrepancies in discretization (see part 5). The 3 variation has a non-convective steady-state solution, as the numerical results show. Here the flow field, which is induced by the upper boundary condition is so strong that hot water does not rise (except from the left vertical boundary, where the overlying flow itself turns upward). There are differences in numerical output concerning the temperature decrease with distance from the source, which are caused by numerical dispersion (see below).

## 5. EFFECTS OF DISCRETIZATION

Differences between the simulations by Yusa [7] and FAST_C(2D) can mostly be attributed to differences in the discretization. Yusa used a finer grid (200 × 40 blocks) on a mainframe and applied central-in-space (CIS) finite differencing for the 1.order terms.

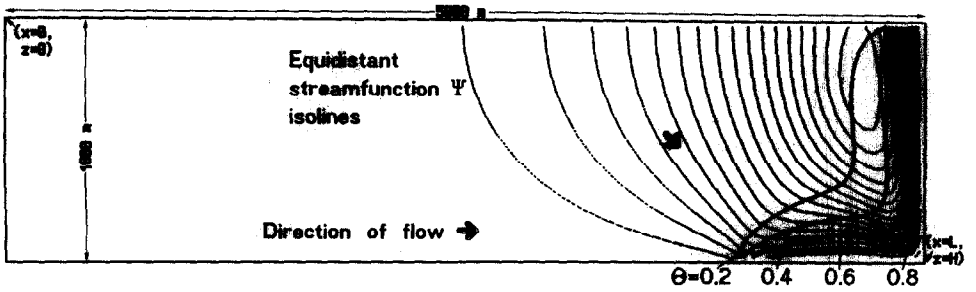


Fig. 5. Steady-state solution of reference case with variable viscosity.

The disadvantage of the CIS-method is that there arise stability problems, while the BIS-(backward-in-space) or upwind-scheme is unconditionally stable. The latter, which is implemented in FAST__C(2D) code, introduces increased numerical dispersion $E$ into the system. The first order approximation of numerical dispersion (truncation error) in the $x$-direction is $v_x\Delta x/2$ [12]—analogous for the $z$-direction: $v_z\Delta z/2$. Thus at the top boundary $E$ becomes 0.245 for the 1 variation, 0.738 for the 2 variation and 1.225 for the 3 variation cases [in the dimensionless system (X)]. These values have to be added to diffusivity $\kappa = 1$ in the transformed system.

Thus the diffusion–dispersion of the physical system, simulated by FAST__C(2D), is much higher. This explains why transients vanish much earlier and why temperature decrease from the source in the upwind scheme simulations is higher—even in hot spots.

## 6. EFFECT OF CHANGING VISCOSITY

It was remarked already by Kassoy and Zebib [13] and later by Straus and Schubert [14], that viscosity varies tremendously in the mentioned temperature range. Additional simulations were done with FAST__C(2D) to examine whether it makes a difference when viscosity changes are taken into account. It is assumed that $Ra$ is determined further on with the same reference value for dynamic viscosity $\mu_{ref}$.

Then the equation

$$\operatorname{div}(\operatorname{grad}\Psi) = \gamma Ra\frac{\mu_{ref}}{\mu}\frac{\partial\Theta}{\partial x}$$

replaces the first equation of (X). Within the simulations $\mu$ is evaluated as a function of $\Theta$:

$$\mu(\Theta) = \mu_{ref}\exp\{a[1/(\Theta+\Theta_0)-1/(\Theta_{ref}+\Theta_0)]\}.$$

With $a = 4$ and $\Theta_0 = -0.652$ the values calculated by this formula are close to those used by Yano [11]. The curve does not deviate much from the one given for fresh water head and saturation pressure in the JSME steam tables [15]. Calculations were done for the reference case and the three variations using FAST__C(2D) with the same spatial and temporal discretizations as used in the constant viscosity case. The results for 5000 years simulation time are given in Figs. 5–8.

Comparison with the constant viscosity simulation shows some deviations in details, but the classification as shown above remains valid with only one exception. In the 1 variation a second hot water plume does not rise along the vertical boundary above the heat source. Therefore the steady-state pattern shows two convection cells only—instead of three in the constant viscosity case.

Yano [11] presented results for the reference case with variable viscosity. In the transient case his solutions have four convective eddies above the geothermal source. In steady state two cells remain with ascending hot water above the free (here left) edge of the source. The patterns are different from the results calculated with constant viscosity by all codes and they differ from the results of FAST__C(2D) with variable viscosity. It is remarkable that the steady-state two-cell pattern of Yano's variable $\mu$ simulation for the reference case resembles very much the output of FAST__C(2D) calculation with variable $\mu$ for the 1 variation.

## 7. CONCLUSIONS

Numerical simulations with FAST__C(2D) code confirm results given before by Yusa [7]. Comparison of the free convection case with variations of free and forced convection shows different flow patterns for all four cases. It is obvious that the Rayleigh number is not the only parameter characterizing mixed convection as stated by Prats [6]. The ratio between the flow introduced by an outer force and buoyancy has to be considered additionally.

In pure fluid applications with density gradients a comparison can be made between buoyancy and inertia terms in the Euler equation of motion

$$\rho\frac{\mathrm{d}\mathbf{v}}{\mathrm{d}t} = -\operatorname{grad}p+\Delta\rho\mathbf{g}$$

where $p$ is dynamic pressure [3]. This leads to a dimensionless Richardson number! To derive a characteristic parameter combination with analogous meaning for the porous media case it is convenient to compare the same two terms in the corresponding equation:

$$\frac{\rho}{\phi}\frac{\partial\mathbf{v}}{\partial t}+\frac{\mu}{k}\mathbf{v} = -\operatorname{grad}p+\Delta\rho\mathbf{g} \qquad (Y)$$

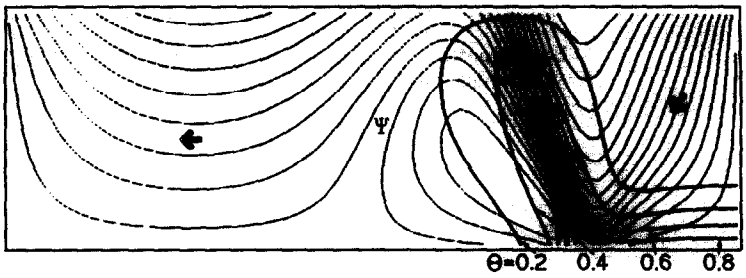


Fig. 6. Steady-state solution of 1 variation with variable viscosity.

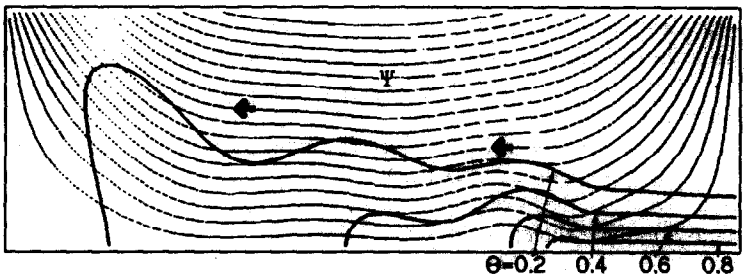


Fig. 7. Transient solution of 2 variation with variable viscosity.

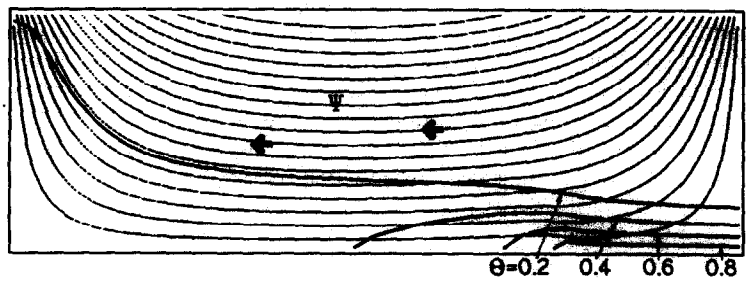


Fig. 8. Steady-state solution of 3 variation with variable viscosity.

[16] or—if time derivative of $v$ is omitted—in Darcy's Law. In the case of forced convection the pressure gradient should be the one which is prescribed by boundary conditions and which is related to boundary velocity $v_b$ by Darcy's Law.

A new dimensionless constant $Co$ may be introduced by the definition:

$$Co = \frac{\Delta\rho g}{\text{grad}\, p} = \frac{k\Delta\rho g}{\mu v_b} = \frac{k\Delta\rho g H}{\mu\kappa}\frac{\kappa}{v_b H} = \frac{Ra}{Pe}.$$

For a given system the relevant dimensionless constant $Co$ can be related to Rayleigh number and Peclet number ($= v_b H/\kappa$). Evaluation for the cases with constant $\mu$ treated above delivers the results of Table 3.

It has to be noted that for these applications the new dimensionless number does not really compare the two terms on the right hand side of equation (Y), because a horizontal pressure gradient is compared to vertical buoyancy. Nevertheless another grad $p$ would make no sense. The values given above characterize classes with different convection patterns, for which $Co$-intervals should be investigated by further numerical experiments. Simulations with variable viscosity indicate that a two-cell steady state exists, which in the classification scheme should be placed between the reference case and the 1 variation.

*Acknowledgements*—E. Holzbecher is grateful for the support from the Ministry of Education, Science and Culture, Japan, which made the research at the Beppu Geophysical

Table 3. Dimensionless characteristic number for forced and free convection

| | $Co$ | Steady convection flow pattern |
|---|---|---|
| Reference case | $\infty$ | One steady convection cell |
| 1 var. (low velocity) | 20.41 | Three steady convection cells |
| 2 var. (medium velocity) | 6.80 | No steady state |
| 3 var. (high velocity) | 4.02 | No convection |

Research Laboratory, Kyoto University possible from March 1992 to February 1993. Members at the laboratory Drs K. Kitaoka, K. Takemura, Y. Fukuda and S. Osawa are thanked for helpful discussions during the research.

## REFERENCES

1. E. R. Lapwood, Convection of a fluid in a porous medium, *Proc. Cam. Phil. Soci A* **225,** 508–521 (1948).
2. S. Bories, Natural convection in porous media. In *Advances in Transport Phenomena in Porous Media* (Edited by J. Bear and M. Y. Corapcioglu), pp. 77–141. Dordrecht (1989).
3. J. S. Turner, *Buoyancy Effects in Fluids*, Chap. 5. Cambridge (1977).
4. M. A. Combarnous and S. A. Bories, Hydrothermal convection in saturated porous media, *Adv. Hydrosci.* **10,** 231–307 (1975).
5. P. Cheng, Similarity solutions for mixed convection from horizontal impermeable surfaces in saturated porous media, *Int. J. Mass Heat Transfer* **20,** 893–898 (1977).
6. M. Prats, The effect of horizontal fluid flow on thermally induced convection in porous mediums, *J. Geophys. Res.* **71,** 4835–4838 (1966).
7. Y. Yusa, Numerical experiment of groundwater motion under geothermal conditions, *J. Geotherm. Res. Soc. Jap.* **5,** 23–38 (1983).
8. R. A. Wooding, Steady state free thermal convection of liquid in a saturated permeable medium, *J. Fluid Mech.* **2,** 273–285 (1957).
9. J. W. Elder, Steady free convection in a porous medium heated from below, *J. Fluid Mech.* **27,** 29–48 (1967).
10. E. Holzbecher, Numerische Modellierung von Dichteströmungen im porösen Medium, *Inst. Wasserbau der TU Berlin*, Mitteilung 117 (1991).
11. Y. Yano, A practical procedure for vertical two-dimensional hydrothermal simulation by finite element method, *J. Jap. Assoc. Petrol. Engng* **54,** 18–31 (1989).
12. E. Holzbecher, Zur mathematischen Modellierung von Ausbreitungsvorgängen im Grundwasser, *VII. Tagung Mathematische Simulation der Grundwasserentnahmen*, TH Krakov (1988).
13. D. R. Kassoy and A. Zebib, Variable viscosity effects on the onset of convection in porous media, *Phys. Fluids* **18,** 1649–1651 (1975).
14. J. M. Straus and G. Schubert, Thermal convection of water in a porous medium: effects of temperature and pressure dependent thermodynamic and transport properties, *J. Geophys. Res.* **82,** 325–333 (1977).
15. Steam tables. JSME, Tokyo (1968).
16. J. P. Caltagirone, Convection in a porous medium. In *Convective Transport and Instability Phenomena* (Edited by J. Zierep and H. Oertel), pp. 199–232. Karlsruhe (1982).